POLITECNICO DI TORINO
Repository ISTITUZIONALE

Optimisation of the Pendulum Wave Energy Converter With Spline-Based Hull Shape

Original
Optimisation of the Pendulum Wave Energy Converter With Spline-Based Hull Shape / Giannini, G., Giorgi, G., Sirigu, S.A., Giorcelli, F., Rosa-Santos, P., Taveira-Pinto, F., Mattiazzo, G.. - ELETTRONICO. - 7B: Ocean Renewable Energy:(2026). (ASME 2026 45th International Conference on Ocean, Offshore and Arctic Engineering Tokyo (JPN) 7-12 June 2026) [10.1115/omae2026-177382].

Availability:
This version is available at: 11583/3016410 since: 2026-10-07T14:54:29Z

Publisher:
ASME

Published
DOI:10.1115/omae2026-177382

Terms of use:

This article is made available under terms and conditions as specified in the corresponding bibliographic description in the repository

Publisher copyright

(Article begins on next page)

20 November 2026

Check for updates

Proceedings of the ASME 2026 45th International Conference on Ocean, Offshore and Arctic Engineering
OMAE2026
June 7-12, 2026, Tokyo, Japan

OMAE2026-177382

Downloaded from asmedigitalcollection.asme.org/OMAE/proceedings-pdf/OMAE2026/89565/V07BT09A041/7645217/v07bt09a041-omae2026-177382.pdf by guest on 07 October 2026

OPTIMISATION OF THE PENDULUM WAVE ENERGY CONVERTER WITH SPLINE-BASED HULL SHAPE

Gianmaria Giannini[1,2,†,*] Giuseppe Giorgi[1,†] Sergej Antonello Sirigu[1] Filippo Giorcelli[1] Paulo Rosa-Santos[2,3] Francisco Taveira-Pinto[2,3] Giuliana Mattiazzo[1]

[1]Politecnico di Torino, MOREnergy Lab, Torino, Italy
[2]Interdisciplinary Centre for Marine and Environmental Research (CIIMAR), Matosinhos, Portugal
[3]Faculty of Engineering of University of Porto, Porto, Portugal

ABSTRACT

Wave energy offers substantial potential but has yet to reach commercial viability due to high costs and reliability challenges. This study advances the Pendulum Wave Energy Converter (PeWEC), an inertial device featuring a fully enclosed Power Take-Off (PTO) to enhance survivability in harsh marine environments. To improve techno-economic performance, this research introduces a spline-based hull parametrisation, offering greater geometric flexibility than previous simplified arc-based designs.

An upgraded optimisation model is presented, employing a genetic algorithm to minimise the ratio of Capital Expenditure (CapEx) to Annual Energy Production (AEP). The design space encompasses hull geometry, mass distribution, and PTO settings, subject to robust physical constraints. A frequency-domain approach simulates device dynamics across 128 representative sea states for a case study off Pantelleria Island, Italy.

Computational results demonstrate the efficiency of the model, with parallelised runs completing within 96 hours. Comparative analyses indicate that spline-based designs significantly outperform benchmark arc-based geometries. Specifically, the spline parametrisation unlocks up to 33% increase in maximum energy yield compared to the limit of the arc-based designs for a comparable investment. These findings validate that advanced hull shaping is critical for accessing superior techno-economic configurations.

Keywords: Ocean Renewable Energy, Inertial WEC, Geometry Optimisation, Hull Design, Multi-Objective Optimisation, Genetic Algorithm, Techno-Economic Analysis, Frequency-Domain Modelling, AEP

NOMENCLATURE

Symbols

$\mathbf{A}(\omega)$	Hydrodynamic added mass matrix
$\mathbf{B}_{rad}(\omega)$	Hydrodynamic radiation damping matrix
$\mathbf{B}_{pto}$	PTO damping vector
C_{hull}	Cost of the floating hull [€]
F_{obj}	Objective function value
$\hat{\mathbf{F}}_{exc}$	Excitation force vector [N, Nm]
H_s	Significant wave height [m]
$\mathbf{K}_{hyd}$	Hydrostatic stiffness matrix
$\mathbf{K}_{pto}$	PTO stiffness
$\mathbf{M}$	System mass and inertia matrix
P_{avg}	Average absorbed power [W]
$\mathbf{q}$	Generalized displacement vector
S_η	Wave energy spectrum [m^2 s]
T_e	Wave energy period [s]
$T_{gen,max}$	Rated generator torque [Nm]
δ	Hull pitch angle [rad]
ε	Relative pendulum rotation angle [rad]
η_{tot}	Electrical and mechanical efficiency [-]
ω	Wave angular frequency [rad s^{-1}]

Acronyms

aCLR	Annual Capture Length Ratio
aCWR	Annual Capture Width Ratio
AEP	Annual Energy Production [MWh]
BEM	Boundary Element Method
CapEx	Capital of Expenditure [€]
CoP	Capital expenditure over AEP ratio [€/MWh]
GA	Genetic Algorithm
PeWEC	Pendulum Wave Energy Converter
PTO	Power Take-Off
RAO	Response Amplitude Operator
WEC	Wave Energy Converter

[†]Joint first authors
[*]Corresponding author: gianmaria.giannini@polito.it

Copyright © 2026 by ASME; reuse license CC-BY 4.0

1. INTRODUCTION

The global transition toward a carbon-neutral energy portfolio requires a diversification of renewable sources to mitigate the variability of wind and solar power and reduce energy storage requirements. Among the available options, ocean waves offer a dense and highly predictable resource. Although numerous Wave Energy Converter (WEC) concepts have been proposed, none have reached a full commercial development stage. Among the most promising concepts, favoured for their mechanical simplicity and survivability, are Oscillating Water Columns (OWCs), which are particularly suited for fixed-to-shore solutions [1–3]. However, for offshore deployment, where the energy resource is significantly higher and spatial constraints are fewer, point absorbers [4–7] and inertial devices [8–10] are often preferred. But moving offshore introduces severe reliability challenges. To minimise expensive marine maintenance, the Pendulum Wave Energy Converter (PeWEC), investigated in this study, utilises a fully enclosed Power Take-Off (PTO). Typical of inertial WECs, this configuration ensures that sensitive electromechanical components are shielded from the corrosive marine environment [11].

The design process for WECs is inherently a complex task. Historically, common WEC design approaches have been sequential and, therefore, suboptimal: the hull geometry is often defined first based on hydrodynamic principles, followed by the selection of the PTO. However, an effective design requires a holistic approach based on representative wave-to-wire mathematical models [12]. This aspect is critical because the implementation of an energy-maximising control strategy introduces strong nonlinearities and fundamentally alters the dynamic response of the device [13]. As a result, energy absorbed-wise optimal solutions for uncontrolled versus controlled conditions can differ significantly [14]. Furthermore, the hydrodynamic behaviour depends mainly on shape, dimensions, linked to volume and mass, which are the primary drivers of capital cost (CapEx) [15, 16]. Navigating this trade-off between energy production and cost requires Multidisciplinary Design Optimisation (MDO). Yet, a practical implementation of an all-encompassing MDO is challenging due to the vast, multi-dimensional search space. In this context, both the cost function and the physical constraints often behave as 'grey' or 'black' boxes, since the system cannot be described by a single mathematical formula or a simple combination of equations. Consequently, Genetic Algorithms (GAs) have become a common choice. As metaheuristic optimisation codes based on evolutionary theory [17], GAs rely on the "survival-of-the-fittest" principle. They are particularly well-suited for high-dimensionality problems where the mathematical structure of the objective function is unknown or non-differentiable [18]. Thanks to their stochastic nature, GAs favour the identification of global optima, reducing the risk of converging to local minima inherent in deterministic methods. To date, the application of GAs within the wave energy sector has been relatively limited. While other metaheuristic approaches such as particle swarm optimisation or differential evolution exist in the general marine engineering field, their application in wave energy has often been limited to array layout optimisation. Device-specific optimisation has seen limited but notable efforts. Shadman et al. [19] optimised the radius and draft of an archetypal cylinder, while Kurniawan and Moan [20] considered fixed-axis devices of conventional shapes. More recently, efforts have been made to break away from simple primitives; for instance, McCabe [21] attempted to generalize the geometry using B-splines, and Cordonnier et al. [22] proposed a newer optimisation of the SEAREV device (initially optimised in [23]).

This paper extends the existing GA-based MDO model of the PeWEC, developed at the MORE research group of Politecnico di Torino. The primary advancement lies in integrating a spline-based parametrisation for the WEC hull. Previously, the optimisation model relied on a simplified hull geometry defined by basic arcs. By employing a spline-based method, this study provides greater geometric flexibility, making it possible to investigate complex shapes that— as demonstrated, for instance, by Garcia-Teruel [24]—can substantially outperform conventional geometries in terms of hydrodynamic efficiency. The following sections detail the PeWEC device and previous work (Section 2), the mathematical and numerical model setup (Sections 3, 4), the definition of hull parametrisations and applied constraints (Sections 5, 6), the comparative results between the new spline-based hull and previous geometries (Section 7) and conclusions (Section 8).

2. PEWEC DEVICE

The PeWEC is a floating inertial WEC developed by the MORE research group (Politecnico di Torino) and the Italian National Agency for New Technologies, Energy and Sustainable Economic Development (ENEA). It harvests energy from the wave-induced pitch motion of a floating hull. Its architecture consists of a generic hull enclosing a pendulum oscillating around a horizontal hinge. As incident waves pitch the hull, the internal pendulum is excited into oscillation, Figure 1. This relative rotation is converted into electricity by a PTO system (comprising a multistage gearbox and generator) connected to the hinge, which applies torque to extract energy and control the pendulum's response. A key advantage of the PeWEC is that all electromechanical components are housed inside the sealed hull. This isolates sensitive equipment from the corrosive marine environment, significantly enhancing reliability and reducing maintenance compared to devices with external moving parts.

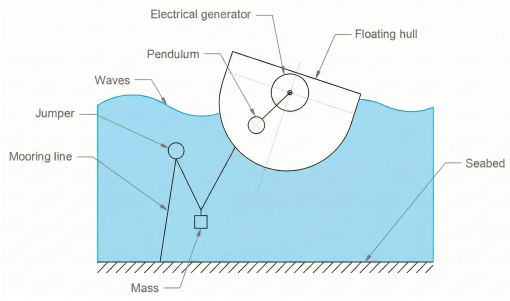


FIGURE 1: Schematic representation of the PeWEC working principle. The relative rotation between the pitching hull and the internal pendulum drives the fully enclosed PTO.

The technological advancement of the PeWEC relies on rigorous numerical modelling and experimental validation. Hydrodynamic testing was conducted at the INSEAN facility (CNR,

Downloaded from asmedigitalcollection.asme.org/OMAE/proceedings-pdf/OMAE2026/89565/V07BT09A041/7645217/v07bt09a041-omae2026-177382.pdf by guest on 07 October 2026

Copyright © 2026 by ASME; reuse license CC-BY 4.0

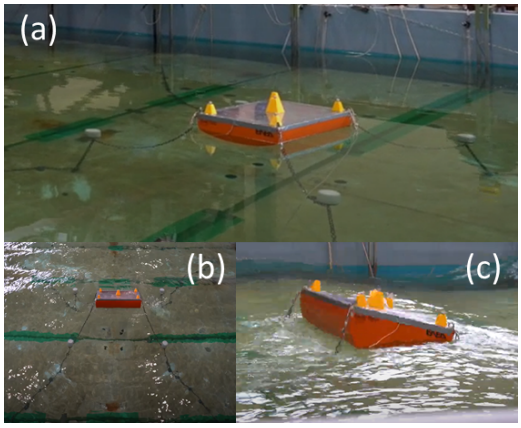


FIGURE 2: Experimental testing of the PeWEC scaled prototype at the wave tank of the University of Naples Federico II, used for numerical model validation.

Rome) [25] and the University of Naples Federico II [26, 27]. The latter, shown in Figure 2, depicts the physical model in calm water (a) and dynamic wave tests (b, c). These campaigns subjected 1:12 and 1:20 scaled prototypes [28] to diverse regular and irregular wave conditions. The empirical data identified non-linear damping contributions [29] and validated the full-scale numerical models [30]. These validated models are now integrated into the holistic optimisation strategy presented in this study.

3. MATHEMATICAL AND NUMERICAL MODELLING

The numerical modelling framework is shown in Figure 3. The process begins by defining the wave energy resource via a site-specific scatter diagram and establishing design space boundaries. An iterative loop evaluates system parameters selected by the algorithm. For each candidate, the model computes hydrodynamic coefficients and assesses power generation using a frequency-domain spectral response model. A constraint handling mechanism applies a "death penalty" to configurations violating physical or geometric limits. This effectively removes infeasible solutions. Finally, a Genetic Algorithm (GA) minimises the objective function to find optimal techno-economic configurations. The model investigates a design space of 16 variables. These include hull geometry, mass distribution, pendulum properties, and PTO settings (torque, velocity, gearbox ratio). Unlike studies using idealized modelling, this approach computes costs based on material consumption and catalogued PTO components [31]. The loop employs a tournament-based NSGA-II algorithm (MI-LXPM) [32]. This handles the high mortality rate caused by strict physical and structural constraints. System dynamics use a spectral-domain approach [33], derived from experimental and numerical validation of the PeWEC [28, 30]. This estimates Annual Energy Production (AEP) rapidly. The objective function minimises the ratio between Capital Expenditure and Annual Energy Production (CapEx/AEP).

3.1. Mathematical model

The device is modelled as a multibody system with a floating hull and internal pendulums oscillating around a horizontal hinge. A frequency-domain approach ensures computational efficiency. This allows the evaluation of thousands of configurations without the high cost of time-domain solvers. A Cartesian reference frame (x, y, z) is defined with the origin at the still water level and the z-axis pointing vertically upwards. Power production analysis focuses on planar motion aligned with the wave direction. The generalized coordinates vector $\mathbf{q}$ describes hull surge (x), heave (z), pitch (δ), and the relative pendulum rotation (ε). The angle ε is the primary degree of freedom for energy extraction, as the PTO couples to the relative motion between the hull and the pendulum. Assuming linear wave theory and small oscillations, the dynamic equilibrium of the coupled system is

$$\begin{aligned}\left[-\omega^2(\mathbf{M}+\mathbf{A}(\omega))+i\omega(\mathbf{B}_{rad}(\omega)+\mathbf{B}_{pto})+\right.\\ \left.(\mathbf{K}_{hyd}+\mathbf{K}_{pto}+\mathbf{K}_{moor})\right]\hat{\mathbf{q}}=\hat{\mathbf{F}}_{exc}(\omega)\end{aligned} \tag{1}$$

where ω denotes wave angular frequency. $\hat{\mathbf{q}}$ and $\hat{\mathbf{F}}_{exc}(\omega)$ are complex amplitudes of displacement and wave excitation force, respectively. $\mathbf{M}$ accounts for mass and inertia of the hull and pendulum, including coupling terms. $\mathbf{A}(\omega)$ and $\mathbf{B}_{rad}(\omega)$ represent added mass and radiation damping. These are computed using the BEM solver Nemoh [34]. Viscous damping is neglected. This is considered acceptable for typical WEC sizes and speeds in operational sea states. $\mathbf{B}_{pto}$ represents linear damping torque applied by the generator. System stiffness includes hydrostatic stiffness $\mathbf{K}_{hyd}$ and PTO stiffness $\mathbf{K}_{pto}$. The latter tunes the resonance frequency. Mooring stiffness $\mathbf{K}_{moor}$ is omitted, being negligible compared to $\mathbf{K}_{hyd}$. For each sea state, optimal $\mathbf{B}_{pto}$ and $\mathbf{K}_{pto}$ are found via a multi-variate simplex algorithm. Crucially, this inner optimisation strictly bounds pendulum stroke and PTO torque to prevent unrealistic responses, rejecting unfeasible combinations.

3.2. Power and Energy Production Estimation

The model quantifies AEP. First, it calculates the Response Amplitude Operator (RAO), $H(\omega)$. Sea states are defined by a wave spectrum $S_\eta(\omega)$, significant wave height H_s, and energy period T_e. The average power absorbed in a sea state is

$$P_{avg}(H_s, T_e) = \int_0^\infty C_{pto}\omega^2 |H_\varepsilon(\omega)|^2 S_\eta(\omega) d\omega \tag{2}$$

where $H_\varepsilon(\omega)$ is the relative pendulum motion RAO. C_{pto} is the scalar PTO damping coefficient extracted from $\mathbf{B}_{pto}$. Total AEP sums the weighted power contributions of all sea states, multiplied by annual hours and an efficiency factor η_{tot}.

4. TECHNO-ECONOMIC METRICS

To evaluate the economic viability of different PeWEC configurations, the optimisation model extends beyond simple hydrodynamic efficiency. The model employs a set of techno-economic metrics that relate the physical performance of the device to its material costs. The primary objective is to minimise the ratio between capital expenditure and AEP. The AEP represents the total electricity generated by the device over one year of operation at the selected deployment site, it is calculated by aggregating the mean power output, $P_{el,i}$, obtained for each sea state i in the scatter diagram, weighted by its probability of occurrence p_i (in

Downloaded from asmedigitalcollection.asme.org/OMAE/proceedings-pdf/OMAE2026/89565/V07BT09A041/7645217/v07bt09a041-omae2026-177382.pdf by guest on 07 October 2026

Copyright © 2026 by ASME; reuse license CC-BY 4.0

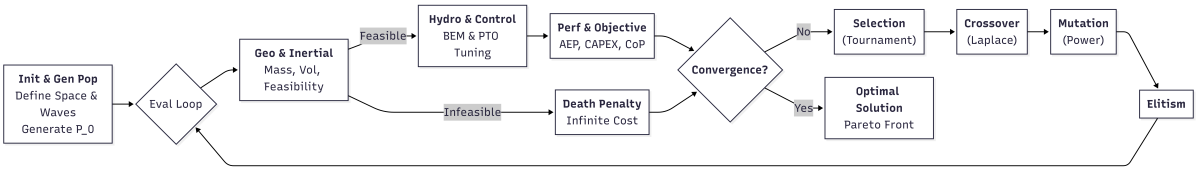


FIGURE 3: Flowchart of the genetic algorithm optimisation model.

hours), Eq. 3.

$$AEP = \eta_{tot} \cdot \sum_{i=1}^{N_{ss}} P_{el,i}(H_{s,i}, T_{e,i}) \cdot p_i \tag{3}$$

where, N_{ss} is the total number of sea states considered, and η_{tot} represents the efficiency of the power and mechanical conversion systems (simplified to the constant value of 0.90). The AEP ensures that the design is optimised for the specific wave climate of the installation site, rather than a theoretical wave climate. The CapEx is estimated using a parametric cost model that links the physical attributes of the device to component costs. Since the device is in a preliminary design phase, costs are aggregated into three main categories: structural steelwork, electromechanical PTO components, and ballast or auxiliary systems, Eq 4.

$$\text{CapEx} = C_{hull} + C_{gen}(T_{gen,max}) + C_{bal} + C_{fix} \tag{4}$$

The structural cost (C_{hull}) constitutes the largest portion of the investment. It is determined by the total mass of the floating hull, which is computed by multiplying the hull's total surface area—derived directly from the geometry function—by a reference steel thickness and material density. A specific unit price for manufactured marine-grade steel is then applied to obtain the total structural value. The PTO cost (C_{gen}) is assessed based on the sizing of the power conversion chain. The model assumes that the investment cost for the PTO group is primarily driven by the rated generator torque ($T_{gen,max}$), as this parameter directly dictates the physical size and volume of the electrical machine. Based on a database of commercial components, a linear regression model is employed. This function aggregates the costs of the entire drivetrain, including the electric generator, multistage gearbox, variable frequency drive, mechanical brake, and encoder. The total cost is composed of a fixed value (c_{base}), representing the baseline cost for the smallest available units, and a variable component scaled by a specific torque coefficient (k_{torque}), which captures the marginal cost increase per unit of torque capacity. Finally, the inertial and ballast costs (C_{bal}) are computed based on the mass required. This calculation distinguishes between the active pendulum mass (metal) and the fixed ballast (concrete or sand) used to adjust the center of gravity. A fixed overhead cost is added to account for assembly, sensors, and other minor subsystems.

4.1. Optimisation Criterion

The optimisation algorithm seeks to minimise a single objective function, the Capital of Expenditure over Productivity ratio (CoP), defined as the ratio of investment cost to energy generation, Eq. 5.

$$CoP = \frac{CapEx}{AEP} \quad \left[\frac{€}{\text{MWh}}\right] \tag{5}$$

By minimising this ratio, the GA naturally selects designs that balance high energy absorption with reasonable dimensions and component ratings. This prevents the selection of physically enormous devices that might capture slightly more energy but would be economically prohibitive to build. The GA parameters shown in Table 1 are set for both hull geometries adopted, ensuring that the comparison between the these two types of hull parametrisation is consistent. The minimisation process of the CoP is driven by the GA with settings detailed in Table 1. A population size of $N_{pop} = 70$ was selected to ensure sufficient diversity and avoid local minima.

TABLE 1: Genetic Algorithm (GA) configuration parameters.

Parameter	Val.	Description
Population Size	70	Number of individuals (design candidates) per generation.
Max Generations	150	Maximum allowed evolutionary iterations.
Max Stall Gen.	150	Termination limit for consecutive generations without fitness improvement.

5. ARC-BASED HULL FORMER PARAMETRISATION

Prior to the introduction of the spline-based method, the optimisation of the PeWEC device relied on a simplified geometric parametrisation, e.g. Figure 4. This approach, detailed in previous studies [11, 31], defined the hull profile using a combination of two arcs. The primary objective was ensuring a design easy to analyse and manufacture while maintaining acceptable hydrodynamics. The hull geometry is generated by extruding a symmetric two-dimensional cross-section along the transverse y-axis, constructed from two tangential arcs: (1) two side arcs with a smaller radius (R_1), located at the bow and stern, connecting the bottom arc to the deck level; and (2) a bottom arc with a large radius (R_2), defining the curvature of the keel.

This configuration ensures a smooth surface with continuous curvature, avoiding sharp edges that could induce vortex shedding or viscous drag losses. Furthermore, the absence of re-entrant angles minimises the risk of slamming events during operation in rough seas. To allow the GA to modify this shape, the geometry was defined by a set of dimensionless parameters rather than explicit coordinates. The overall size is set by the length (L), width (W), and height (H). The specific curvature of the profile is controlled by two shape factors: the bow/stern circumference ratio

Downloaded from asmedigitalcollection.asme.org/OMAE/proceedings-pdf/OMAE2026/89565/V07BT09A041/7645217/v07bt09a041-omae2026-177382.pdf by guest on 07 October 2026

Copyright © 2026 by ASME; reuse license CC-BY 4.0

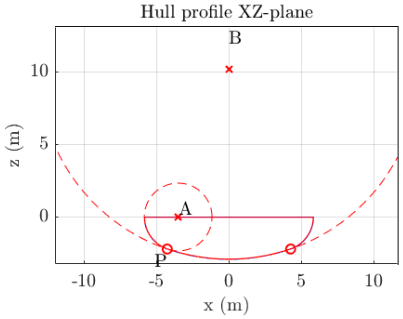


FIGURE 4: Example of arc-based hull and its design building points.

(h), which determines the horizontal position of the side arcs, and the height ratio (k), which relates the hull height to the curvature radius. While this arc-based parametrisation offers a refined mathematical framework and structural simplicity, it inherently limits the design space. The rigid constraint of constant-radius arcs prevents the optimiser from exploring subtle variations in volume distribution that could enhance hydrodynamic coupling. A spline-based approach overcomes these limitations by introducing higher degrees of freedom in the hull profile.

6. B-SPLINE BASED 2D-HULL PARAMETRISATION

The geometric definition of the WEC hull significantly influences its hydrodynamic response and, consequently, its energy absorption capability. A spline-based approach is adopted here to overcome the limitations of simple arc formulation used in previous studies, Figure 5. It allows the optimiser to explore shapes that are better tuned to the local wave climate without being restricted to constant-radius arcs. The hull profile is generated using a cubic B-spline curve, denoted as $S(u)$. The curve is constructed as a weighted sum of control points, where the weights are determined by basis functions, Eq. 6.

$$S(u) = \sum_{i=1}^{6} P_i \cdot B_i(u) \tag{6}$$

In this formulation, u represents a parametric variable ranging from 0 to 1. The terms $P_i = (P_{ix}, P_{iy})$ refer to the control points in the two-dimensional plane. $B_i(u)$ are the cubic B-spline basis functions defined over a knot vector. These basis functions are piecewise polynomials of degree three. They satisfy the unity condition shown in Eq. 7.

$$\sum_{i=1}^{6} B_i(u) = 1 \quad \text{for all } u \in [0, 1] \tag{7}$$

A clamped knot vector is employed. This ensures the generated curve starts exactly at the first control point P_1 and terminates at the last point P_6. Bow-stern symmetry is enforced to reduce the number of control points and enable a direct comparison with the original arc-based hull. The six control points are derived from the overall dimensions of the hull, Length (L) and Height (H), and three dimensionless shape parameters $s_1, s_2, s_3 \in [0, 1]$. The coordinates are calculated as, Eq. 8.

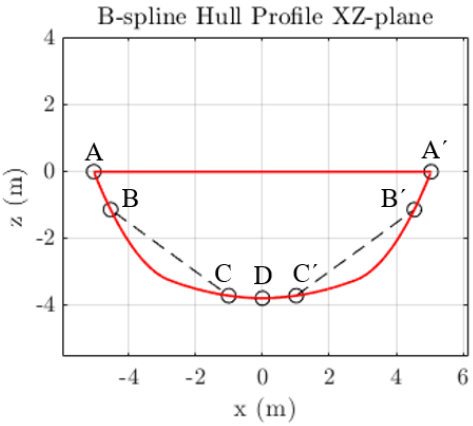


FIGURE 5: Example of spline-based hull and its design building points.

$$\begin{aligned}
A = P_1 &= \left(-\frac{L}{2}, 0\right) \\
B = P_2 &= \left(Ls_1 - \frac{L}{2}, -Hs_2\right) \\
C = P_3 &= \left(Ls_3 - \frac{L}{2}, -H\right) \\
C' = P_4 &= \left(Ls_3 + \frac{L}{2}, -H\right) \\
B' = P_5 &= \left(Ls_1 + \frac{L}{2}, -Hs_2\right) \\
A' = P_6 &= \left(\frac{L}{2}, 0\right)
\end{aligned} \tag{8}$$

This parametrisation effectively reduces the complex problem of shape optimisation to the three variables s_1, s_2, s_3. P_1 and P_6 fix the waterline beam. The intermediate points P_2 and P_5 are the main driver of the curvature of spline (can change in both x and z axes). P_3 and P_4 can change only on the x-axis and depends on H_{draft} (hull draft). While, variables s_1 and s_3 control the horizontal distribution of P_2, P_3, P_4 and P_5 and s_2 modifies the vertical position of P_2 and P_5.

6.1. Spline-based Hull Profile Validation Criteria

GA's selected control points can result in shapes that are mathematically valid but physically impractical for a floating WEC. Strict geometric constraints are necessary to ensure manufacturability and hydrostatic stability. Two primary validity checks are applied to the profile function $S(u)$ representing the internal and external hull surfaces. Any design candidate violating these rules is immediately discarded by the optimisation process.

6.1.1. Monotonicity Constraint: The hull profile must curve consistently to avoid creating pockets or re-entrant shapes that would be difficult to manufacture and hydrodynamically unsuitable (e.g. shapes inducing slamming or excessive drag loads). The first condition enforces monotonicity on the submerged pro-

Downloaded from asmedigitalcollection.asme.org/OMAE/proceedings-pdf/OMAE2026/89565/V07BT09A041/7645217/v07bt09a041-omae2026-177382.pdf by guest on 07 October 2026

Copyright © 2026 by ASME; reuse license CC-BY 4.0

file from the waterline to the keel. For the left half of the symmetric hull ($x \in [-L/2, 0]$), the slope of the profile must never be positive. The mathematical formulation for this constraint is provided in Eq. 9.

$$f'(x) \leq 0 \quad \text{for all } x \in \left[-\frac{L}{2}, 0\right] \tag{9}$$

This derivative condition is verified by evaluating the B-spline at discrete intervals along the curve. The model verifies that for every step from the waterline downwards (from the left to the centre of the hull), the vertical coordinate does not increase, and the horizontal coordinate rises progressively toward the centreline.

6.1.2. Geometric Consistency and Height Constraint: The second constraint ensures the relative vertical positioning of the control points remains consistent. The parameter s_2 controls the vertical position of the intermediate point P_2. If P_2 were allowed to drop below P_3 (the bottom of the hull), the resulting curve would produce a keel extending deeper than the intended draft H. Conversely, if P_2 is placed too high, it creates an excessively sharp corner at the waterline. Therefore, the vertical coordinate of P_2 is constrained to lie strictly between the waterline and the draft. This is enforced by the bounds on s_2 and an additional check shown in Eq. 10.

$$0 \geq P_{2y} \geq P_{3y} \tag{10}$$

This condition guarantees the hull maintains a convex or semi-convex shape appropriate for a pitching body. Furthermore, this constraint indirectly secures sufficient internal volume for the pendulum swing. With additional geometry numerical checks, it is prevented that the hull walls curve excessively inward. The model also ensures the internal cavity remains large enough to house the PTO mechanism and ballasts.

7. RESULTS

The optimisation model evaluated two distinct hull parametrisations: the benchmark arc-based geometry and the proposed spline-based one. The reference wave climate is the offshore site of Pantelleria Island, Italy, selected for its high energy potential and need for on-site energy solutions. Table 2 summarizes the boundaries for the optimisation variables, which rely on preliminary sensitivity analyses and historical data from previous PeWEC studies. Variables cover general hull dimensions, shape coefficients, inertial mass distribution, and PTO settings. The ranges are intentionally broad to allow the GA to explore unconventional designs, while strict upper bounds ensure compatibility with manufacturing, transport, and port infrastructure.

The computational effort for GA simulations was significant, with each full run taking approximately 96 hours on a high-end workstation. The most time-consuming step was the Nemoh code execution for calculating hydrodynamic coefficients. To manage constraints and reduce the impact of infeasible solutions, the NSGA-II effectively stabilized the population. Figure 6 illustrates the mortality rate for both hull types, representing the percentage of individuals failing to meet physical or geometric requirements per generation. The arc-based optimisation started

TABLE 2: Boundaries and definitions of the design variables for the optimisation problem.

Variable	Range	Unit	Description
General Hull Parameters			
Length (L)	$[10, 30]$	m	Hull length parameter.
Width (W)	$[5, 25]$	m	Hull width ratio.
Draft param (α)	$[15, 25]$	deg	Hull draft parameter.
Height Ratio (k)	$[0.4, 1.0]$	-	Hull height ratio.
Arc Hull Specific			
Shape Ratio h	$[0.4, 1.0]$	-	Hull shape ratio.
Spline Hull Specific			
s_1	$[0.0, 0.2]$	-	Hull spline parameter 1.
s_2	$[0.15, 0.8]$	-	Hull spline parameter 2.
s_3	$[0.2, 0.5]$	-	Hull spline parameter 3.
Inertial & Ballast			
Ballast (BFR)	$[0.1, 1.0]$	-	Ballast filling ratio.
Inertia (J_p)	$[5, 30] \cdot 10^3$	kg m^2	Pendulum mass/inertia.
Arm (l_p)	$[0.5, 5.0]$	m	Pendulum arm length.
Shape W/L	$[0.5, 2.5]$	-	Pendulum shape factor (width/length).
Shape H/L	$[0.45, 2.5]$	-	Pendulum shape factor (height/length).
System Setup			
Pendulums (n)	$[1, 4]$	-	Number of pendulums.
PTO ID	$[1, 37]$	-	PTO identification number.

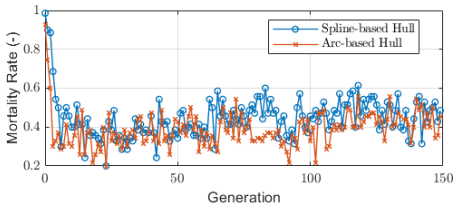


FIGURE 6: Mortality rate comparison: spline vs arc-based hull GA optimisation runs.

with a 93% mortality rate, dropping to 30% by the third generation. The spline-based optimisation began at 99%, reflecting the difficulty of randomly generating valid spline shapes, but stabilized between 30% and 50%. The persistent mortality in later generations indicates the algorithm continues pushing design boundaries rather than stagnating in safe, suboptimal local minima.

To understand the physical drivers behind the numerical results, Table 3 details the characteristics of high-performing individuals (5th ranked by CoP). The spline-based optimiser converged toward a more slender hull configuration, featuring slightly greater length (19.99 m) but significantly reduced width (7.56 m) compared to the arc-based design (18.74 m and 9.19 m). This indicates that spline parametrisation allows finer hydrodynamic tuning without requiring a large waterplane area. A narrower beam directly reduces structural steel mass and CapEx. Furthermore, the Ballast Filling Ratio (BFR) differs notably. The spline design has a BFR of 0.13 compared to 0.30 for the arc design, indicating that the spline geometry possesses better hydrostatic properties, reducing the need for deadweight ballasts. The op-

Downloaded from asmedigitalcollection.asme.org/OMAE/proceedings-pdf/OMAE2026/89565/V07BT09A041/7645217/v07bt09a041-omae2026-177382.pdf by guest on 07 October 2026

Copyright © 2026 by ASME; reuse license CC-BY 4.0

TABLE 3: Design parameters of the selected optimal individuals (5th lowest CoP) for Arc-based and Spline-based geometries.

Geometry	L [m]	W [m]	α [deg]	k [-]	h [-]	s_1 [-]	s_2 [-]	s_3 [-]	BFR [-]	J_p [kg m^2]	l_p [m]	$Sh_{W/L}$ [-]	$Sh_{H/L}$ [-]	n [-]	PTO ID
Arc-based	18.74	9.19	24.9	0.99	0.51	–	–	–	0.30	29371	2.38	1.71	0.49	1	10
Spline-based	19.99	7.56	15.5	1.00	–	0.15	0.22	0.46	0.13	28489	2.60	1.23	0.79	1	10

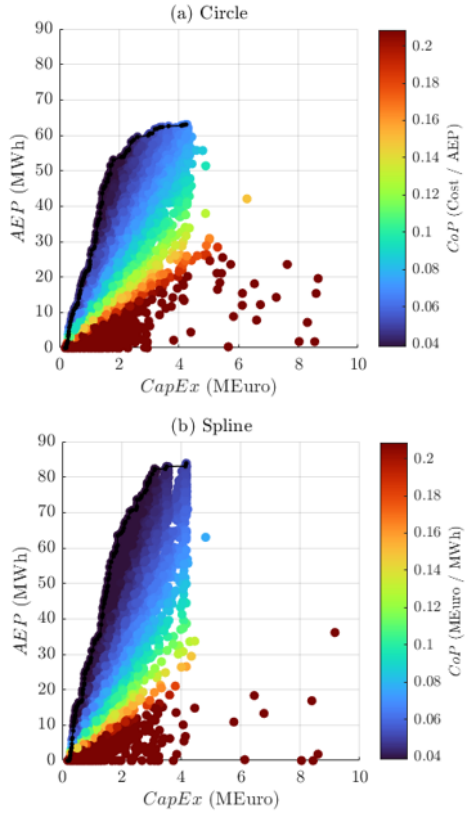


FIGURE 7: Coefficient of Performance: (a) results for former arc-based hull; (b) results for spline-based hull.

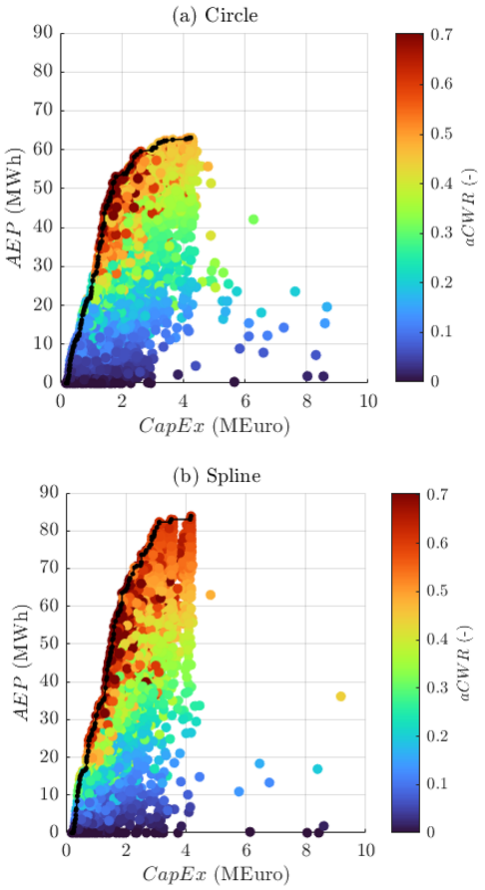


FIGURE 8: Annual Capture Width Ratio: (a) results for former arc-based hull; (b) results for spline-based hull.

timisation also affected internal pendulum parameters. While pendulum inertia (J_p) remains comparable ($\approx$ 29,000 kg m^2), the spline-based solution adopted a longer arm (2.60 m vs 2.38 m), suggesting the spline hull is tuned to a lower frequency band. Both optimisations selected the same PTO unit (ID 10), indicating generator sizing is driven primarily by the Pantelleria wave resource power density rather than hull parametrisation. The algorithm finds a larger generator would not be utilised often enough to justify the cost.

The primary metric for this study is the CoP. Figure 7 maps the population in terms of AEP versus CapEx. The color gradient represents the CoP value, with darker colors indicating more efficient designs. The plot demonstrates a smooth gradient where CoP decreases as the design moves toward higher AEP and lower cost. The difference between the two populations is distinct. The arc-based best individuals generally provide an AEP between 30 and 60 MWh with costs between 1.5 and 2.3 M€. The "Pareto front" for the arc geometry is limited to around 60 MWh. In contrast, the spline-based population expands the feasible design space, identifying configurations with CoP below 0.04, AEP up to 80 MWh, and costs ranging from 1.5 to 2.5 M€. Crucially, for a similar upper-bound investment, the spline-based parametrisation allows a 33% increase in AEP capacity (from 60 to 80 MWh) compared to the arc-based saturation point, extending design regions with higher energy yield potential.

Figure 8 illustrates the Annual Capture Width Ratio (aCWR). The arc-based geometry limits the optimal AEP to a band between 45 and 55 MWh. Conversely, the spline-based results show a broader distribution, with maxima ranging from 30 to 70 MWh. This spread suggests that spline parametrisation offers greater flexibility, allowing the optimiser to find a larger variety of near-optimal configurations suitable for specific site characteristics.

To normalize performance against device length, Figure 9 shows the aCLR. The spline-based hull achieves significantly higher aCLR values, approximately 0.2 higher than the arc-based equivalent. Physically, this indicates that for a set L the spline shape generates hulls with better coupling to the wave pitch moment, converting wave slope into hull rotation more efficiently.

Downloaded from asmedigitalcollection.asme.org/OMAE/proceedings-pdf/OMAE2026/89565/V07BT09A041/7645217/v07bt09a041-omae2026-177382.pdf by guest on 07 October 2026

Copyright © 2026 by ASME; reuse license CC-BY 4.0

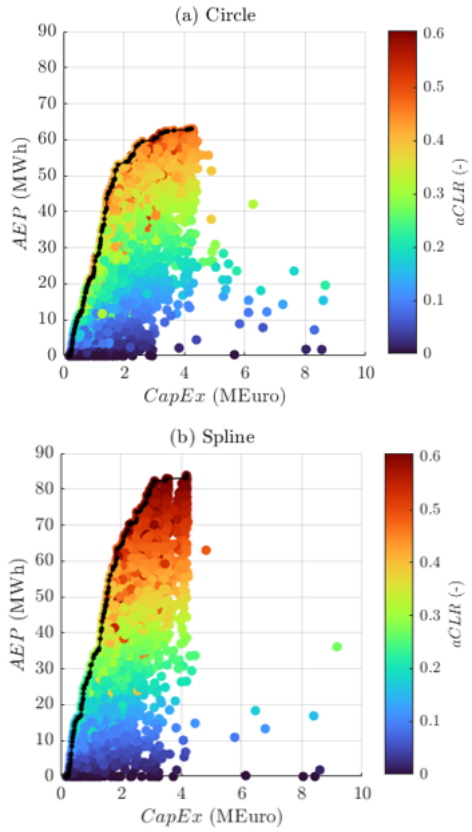


FIGURE 9: Annual Capture Length Ratio: (a) results for former arc-based hull; (b) results for spline-based hull.

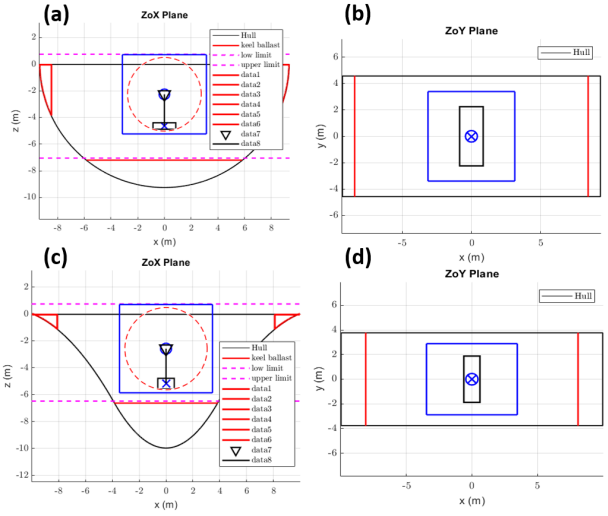


FIGURE 10: Example of optimal hulls shapes: (a) side view with design elements and bounds of an arc-based hull; (b) relative top view of the arc-based hull; (c) side view with design elements and bounds of an spline-based hull; (d) relative top view of the spline-based hull.

Figure 10 visualises the layout of optimal individuals. The bounding boxes indicate strict geometric constraints for the PTO, ballast, and pendulum trajectory. The visual comparison highlights the difference in wall slope and bottom curvature; the arc-based hull (a) is constrained to a rounded bottom, while the spline-based hull (c) adopts sharper bow and stern profiles.

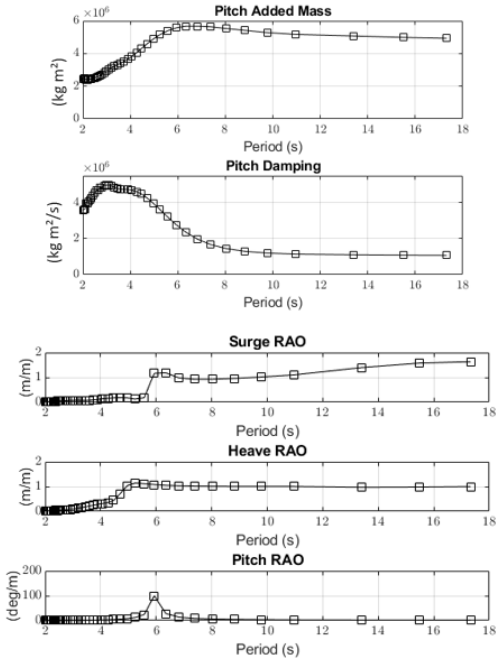


FIGURE 11: Pitch added mass, radiation damping and RAOs for the arc-based hull.

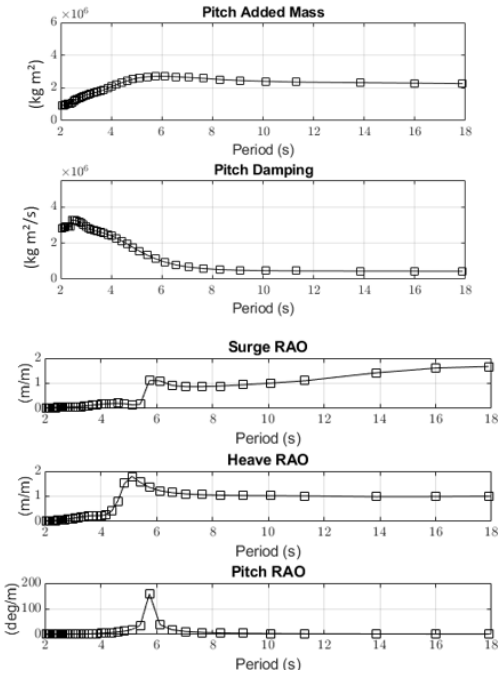


FIGURE 12: Pitch added mass, radiation damping and RAOs for the spline-based hull.

Finally, Figures 11 and 12 shows hydrodynamic coefficients and RAOs for the arc and spline-based hulls, respectively. Both pitch added mass and radiation damping are lower for the spline hull. A lower radiation damping indicates the hull is less damped

Copyright © 2026 by ASME; reuse license CC-BY 4.0

Downloaded from asmedigitalcollection.asme.org/OMAE/proceedings-pdf/OMAE2026/89565/V07BT09A041/7645217/v07bt09a041-omae2026-177382.pdf by guest on 07 October 2026

by its own motion. Consequently, the pitch RAO peak is higher and narrower for the spline-based design. This increased resonant response is likely the primary factor contributing to superior energy capture, as the hull acts as a higher-quality resonator.

8. CONCLUSIONS

This study advances PeWEC techno-economic optimisation by minimising the CapEx over Productivity ratio (CoP) for a Pantelleria Island case study. A genetic algorithm coupled with a frequency-domain model navigated the design space, by means of a cubic B-spline hull parametrisation to replace rigid arc-based geometries.

Comparative analysis shows spline-based designs reach an AEP of 30–80 MWh for 1.5–2.5 M€, surpassing arc-based limits (30–60 MWh at 1.5–2.3 M€). This unlocks a 33% AEP gain for a comparable investment. Splines improve the Annual Capture Length Ratio (aCLR) by approximately 0.2. These slender spline shapes reduce unnecessary volume, lowering pitch added mass and radiation damping, thereby significantly enhancing the resonant pitch RAO.

While the frequency-domain approach neglects non-linear viscous and mooring effects, its computational efficiency is absolutely vital for evaluating thousands of design candidates in a practical time-frame. Although these linear assumptions require subsequent high-fidelity time-domain and physical validation, the spline-based formulation shows to be advantageous for early-stage exploration. Future work will include nonlinear hydrodynamics, PTO efficiency mappings alongside higher-order and asymmetric spline profiles.

9. ACKNOWLEDGEMENTS

This study was made possible thanks to funding from the European Research Executive Agency (REA) under the European Union's Horizon Europe research and innovation programme through the Marie Skłodowska-Curie grant agreement No. 101206509 - Project WEC-Pro. Additional support was previously provided to GG's work through the Stimulus of Scientific Employment programme of the Portuguese Fundação para a Ciência e a Tecnologia (FCT), under the individual grant reference 2022.04954.CEECIND/CP1728/CT0007.

REFERENCES

[1] Heath, T. V. "A review of oscillating water columns." *Philosophical Transactions of the Royal Society A: Mathematical, Physical and Engineering Sciences* Vol. 370 No. 1959 (2012): pp. 235–245. DOI 10.1098/rsta.2011.0164.

[2] Falcão, António F. O. and Henriques, João C. C. "Oscillating-water-column wave energy converters and air turbines: A review." *Renewable Energy* Vol. 85 (2016): pp. 1391–1424. DOI https://doi.org/10.1016/j.renene.2015.07.086.

[3] Portillo, J. C. C., Collins, K. M., Gomes, R. P. F., Henriques, J. C. C., Gato, L. M. C., Howey, B. D., Hann, M. R., Greaves, D. M. and Falcão, A. F. O. "Wave energy converter physical model design and testing: The case of floating oscillating-water-columns." *Applied Energy* Vol. 278 (2020): p. 115638. DOI https://doi.org/10.1016/j.apenergy.2020.115638.

[4] Falnes, Johannes and Hals, Jørgen. "Heaving buoys, point absorbers and arrays." *Philosophical Transactions of the Royal Society A: Mathematical, Physical and Engineering Sciences* Vol. 370 No. 1959 (2012): pp. 246–277. DOI 10.1098/rsta.2011.0249.

[5] Giannini, G., Day, S., Rosa-Santos, P. and Taveira-Pinto, F. "A Novel 2-D Point Absorber Numerical Modelling Method." *Inventions* Vol. 6 No. 4 (2021): p. 75.

[6] Rava, Marcello, Dafnakis, Panagiotis, Martini, Vittorio, Giorgi, Giuseppe, Orlando, Vincenzo, Mattiazzo, Giuliana, Bracco, Giovanni and Gulisano, Andrea. "Low-Cost Heaving Single-Buoy Wave-Energy Point Absorber Optimization for Sardinia West Coast." *Journal of Marine Science and Engineering* Vol. 10 No. 3 (2022): p. 397. DOI 10.3390/jmse10030397. Accessed 2026-01-30, URL https://www.mdpi.com/2077-1312/10/3/397.

[7] Giannini, Gianmaria, Giorgi, Giuseppe, Santos, Paulo, Taveira-Pinto, Francisco, Mattiazzo, G., Ramos, Victor and Giorcelli, Ermanno. "Multi-Objective Development of a Point Absorber Wave Energy Converter Using Dynamic Modelling." *Proceedings of the European Wave and Tidal Energy Conference* Vol. 16 (2025). DOI 10.36688/ewtec-2025-1128.

[8] Boren, B. C., Batten, B. A. and Paasch, R. K. "Active control of a vertical axis pendulum wave energy converter.": pp. 1033–1038. 2014. DOI 10.1109/ACC.2014.6859459.

[9] Nicola, Pozzi, Giovanni, Bracco, Biagio, Passione, Antonello, Sirigu Sergej, Giacomo, Vissio, Giuliana, Mattiazzo and Gianmaria, Sannino. "Wave Tank Testing of a Pendulum Wave Energy Converter 1:12 Scale Model." *International Journal of Applied Mechanics* Vol. 09 No. 02 (2017): p. 1750024. DOI 10.1142/S1758825117500247.

[10] Khedkar, Kaustubh, Nangia, Nishant, Thirumalaisamy, Ramakrishnan and Bhalla, Amneet Pal Singh. "The inertial sea wave energy converter (ISWEC) technology: Device-physics, multiphase modeling and simulations." *Ocean Engineering* Vol. 229 (2021): p. 108879. DOI https://doi.org/10.1016/j.oceaneng.2021.108879.

[11] Pozzi, Nicola, Bracco, Giovanni, Passione, Biagio, Sirigu, Sergej Antonello and Mattiazzo, Giuliana. "PeWEC: Experimental validation of wave to PTO numerical model." *Ocean Engineering* Vol. 167 (2018): pp. 114–129. DOI 10.1016/j.oceaneng.2018.08.028. Accessed 2025-11-27, URL https://www.sciencedirect.com/science/article/pii/S0029801818315233.

[12] Penalba, M. and Ringwood, J.V. "A high-fidelity wave-to-wire model for wave energy converters." *Renewable Energy* Vol. 134 (2019): pp. 367–378. DOI 10.1016/j.renene.2018.11.040.

[13] Ringwood, J.V., Merigaud, A., Faedo, N. and Fusco, F. "An Analytical and Numerical Sensitivity and Robustness Analysis of Wave Energy Control Systems." *IEEE Transactions on Control Systems Technology* Vol. 28 (2019): pp. 1337–1348. DOI 10.1109/TCST.2019.2905060.

Downloaded from asmedigitalcollection.asme.org/OMAE/proceedings-pdf/OMAE2026/89565/V07BT09A041/7645217/v07bt09a041-omae2026-177382.pdf by guest on 07 October 2026

Copyright © 2026 by ASME; reuse license CC-BY 4.0

[14] Garcia-Rosa, P., Bacelli, G. and Ringwood, J. "Control-Informed Geometric Optimization of Wave Energy Converters: The Impact of Device Motion and Force Constraints." *Energies* Vol. 8 (2015): pp. 13672–13687. DOI 10.3390/en81212386.

[15] Farrell, N., Donoghue, C. and Morrissey, K. "Quantifying the uncertainty of wave energy conversion device cost for policy appraisal: An Irish case study." *Energy Policy* Vol. 78 (2015): pp. 62–77. DOI 10.1016/j.enpol.2014.12.022.

[16] Giannini, G., Rosa-Santos, P., Ramos, V. and Taveira-Pinto, F. "Wave energy converters design combining hydrodynamic performance and structural assessment." *Energy* (2022).

[17] Emmerich, M.T. and Deutz, A.H. "A tutorial on multiobjective optimization: Fundamentals and evolutionary methods." *Natural Computing* Vol. 17 (2018): pp. 585–609. DOI 10.1007/s11047-018-9685-y.

[18] Deb, K. "An efficient constraint handling method for genetic algorithms." *Computer Methods in Applied Mechanics and Engineering* Vol. 186 (2000): pp. 311–338. DOI 10.1016/S0045-7825(99)00389-8.

[19] Shadman, M., Estefen, S.F., Rodriguez, C.A. and Nogueira, I.C. "A geometrical optimization method applied to a heaving point absorber wave energy converter." *Renewable Energy* Vol. 115 (2018): pp. 533–546. DOI 10.1016/j.renene.2017.08.055.

[20] Kurniawan, A. and Moan, T. "Optimal geometries for wave absorbers oscillating about a fixed axis." *IEEE Journal of Oceanic Engineering* Vol. 38 (2013): pp. 117–130. DOI 10.1109/JOE.2012.2208666.

[21] McCabe, A.P. "Constrained optimization of the shape of a wave energy collector by genetic algorithm." *Renewable Energy* Vol. 51 (2013): pp. 274–284. DOI 10.1016/j.renene.2012.09.054.

[22] Cordonnier, J., Gorintin, F., Cagny, A. De, Clément, A. H. and Babarit, A. "SEAREV: Case study of the development of a wave energy converter." *Ren. Energy* Vol. 80 (2015): pp. 40–52.

[23] Babarit, A., Clément, A. H. and Gilloteaux, J. C. "Optimization and time-domain simulation of the SEAREV wave energy converter." *Proceedings of the 24th International Conference on Offshore Mechanics and Arctic Engineering* Vol. 2 (2005): pp. 703–712.

[24] Garcia-Teruel, Anna and Forehand, David I. M. "Manufacturability considerations in design optimisation of wave energy converters." *Renewable Energy* Vol. 187 (2022): pp. 857–873. DOI 10.1016/j.renene.2021.12.145. Accessed 2025-11-27, URL https://www.sciencedirect.com/science/article/pii/S0960148121018747.

[25] Pozzi, N., Bracco, G., Passione, B., Sirigu, S.A., Vissio, G., Mattiazzo, G. and Sannino, G. "Wave Tank Testing of a Pendulum Wave Energy Converter 1:12 Scale Model." *International Journal of Applied Mechanics* Vol. 9 (2017): p. 1750024.

[26] Sirigu, S.A., Bonfanti, M., Passione, B., Begovic, E., Bertorello, C., Dafnakis, P., Bracco, G., Giorcelli, E. and Mattiazzo, G. "Experimental investigation of the hydrodynamic performance of the ISWEC 1:20 scaled device." *Proceedings of the NAV International Conference on Ship and Shipping Research*: pp. 551–560. 2018. Trieste, Italy.

[27] Sirigu, A. Sergej, Bonfanti, Mauro, Begovic, Ermina, Bertorello, Carlo, Dafnakis, Panagiotis, Giorgi, Giuseppe, Bracco, Giovanni and Mattiazzo, Giuliana. "Experimental Investigation of the Mooring System of a Wave Energy Converter in Operating and Extreme Wave Conditions." *Journal of Marine Science and Engineering* Vol. 8 No. 3 (2020). DOI 10.3390/jmse8030180.

[28] Pozzi, N., Bracco, G., Passione, B., Sirigu, S.A. and Mattiazzo, G. "PeWEC: Experimental validation of wave to PTO numerical model." *Ocean Engineering* Vol. 167 (2018): pp. 114–129. DOI 10.1016/j.oceaneng.2018.08.028.

[29] Fontana, M., Casalone, P., Sirigu, S.A. and Giorgi, G. "Viscous Damping Identification for a Wave Energy Converter Using CFD-URANS Simulations." *Journal of Marine Science and Engineering* Vol. 8 (2020): p. 355. DOI 10.3390/jmse8050355.

[30] Pozzi, N. "Numerical Modeling and Experimental Testing of a Pendulum Wave Energy Converter (PeWEC)." Ph.D. Thesis, Polytechnic of Turin, Torino, Italy. 2018.

[31] Sirigu, Sergej A., Foglietta, Ludovico, Giorgi, Giuseppe, Bonfanti, Mauro, Cervelli, Giulia, Bracco, Giovanni and Mattiazzo, Giuliana. "Techno-Economic Optimisation for a Wave Energy Converter via Genetic Algorithm." *Journal of Marine Science and Engineering* Vol. 8 No. 7 (2020). DOI 10.3390/jmse8070482.

[32] Deb, K., Pratap, A., Agarwal, S. and Meyarivan, T. "A fast and elitist multiobjective genetic algorithm: NSGA-II." *IEEE Transactions on Evolutionary Computation* Vol. 6 No. 2 (2002): pp. 182–197. DOI 10.1109/4235.996017. Accessed 2025-11-27, URL https://ieeexplore.ieee.org/document/996017.

[33] Bonfanti, Mauro and Sirigu, Sergej Antonello. "Spectral-domain modelling of a non-linear wave energy converter: Analytical derivation and computational experiments." *Mechanical Systems and Signal Processing* Vol. 198 (2023): p. 110398. DOI 10.1016/j.ymssp.2023.110398. Accessed 2025-11-27, URL https://www.sciencedirect.com/science/article/pii/S0888327023003059.

[34] Babarit, A. "Nemoh - url: lheea.ec-nantes.fr." Website. 2014.

Downloaded from asmedigitalcollection.asme.org/OMAE/proceedings-pdf/OMAE2026/89565/V07BT09A041/7645217/v07bt09a041-omae2026-177382.pdf by guest on 07 October 2026

 Copyright © 2026 by ASME; reuse license CC-BY 4.0